Experimental investigation of the robustness of partially entangled qubits over 11 km

R. T. Thew,[1] S. Tanzilli,[1,2] W. Tittel,[1,3] H. Zbinden,[1] and N. Gisin[1]
[1]*Group of Applied Physics, University of Geneva, 1211 Geneva 4, Switzerland*
[2]*Laboratoire de Physique de la Matière Condensée, CNRS UMR 6622, Université de Nice-Sophia Antipolis, Parc Vadose, 06108 Nice Cedex 2, France*
[3]*Danish Quantum Optics Center, Institute for Physics and Astronomy, University of Aarhus, Denmark*
(Received 10 July 2002; published 6 December 2002)

We experimentally investigate time-bin qubits for distributed quantum communication. The robustness of maximal and nonmaximal time-bin entangled qubits (photons) over distances up to 11 km is shown. The entanglement is set by controllable parameters and in all cases is found to be robust, in that the qubits maintain their degree of entanglement after transmission along telecommunication fiber.

DOI: 10.1103/PhysRevA.66.062304 PACS number(s): 03.67.Hk, 03.65.Ud, 03.67.Lx, 42.50.Ar

I. INTRODUCTION

Quantum communication and quantum networks are only part of a much larger field now of quantum-information science [1]. At the heart of many of these associated endeavors is entanglement [2]. Entangled states also play an essential role with respect to the fundamental nature of the microscopic world as investigated in tests of Bell inequalities [3–7]. Beyond the mere existence of entanglement, quantum communication schemes like quantum cryptography [8,9] and teleportation [10–13] have been developed to utilize what has become known as this *quantum resource* entanglement. Schemes using photonic quantum channels that connect distant nodes of a quantum network [14] or for quantum repeaters [15] rely on the possibility to broadcast entanglement over significant distances.

An important aspect which has received little attention from an experimental perspective is that information may need to be encoded in possibly unknown states of arbitrary degrees of entanglement. Finding a means of generating and distributing these states is necessary for progress in this field. Today, the longest reported transmission of entangled qubits is of 360 m [16]. However, this experiment relied on polarization entanglement that is difficult to transmit over long distances of optical fibers due to (polarization mode) dispersion effects. We have previously shown that maximally energy-time entangled photons are robust enough to violate a Bell inequality between analyzers 10 km apart [6]. These, however, are not true qubits and only maximally entangled states were considered. In this article, we investigate the robustness of partially, and maximally, entangled time-bin qubits, when transmitted over optical fibers of up to 11 km, along the way providing the necessary basis for distribution of arbitrary states. We will consider a state to be robust if the initial entanglement is unchanged over the length of the transmission.

Another motivation revolves around the suggestion that the entangled states, when transmitted over appreciable distances, may *spontaneously collapse* onto one of its factors [17,18], with respect to the Schmidt basis. The Schmidt basis uniquely defines the nonmaximally entangled states. In this framework the maximally entangled state would, due to its inherent symmetry, be more stable, before collapsing randomly onto one of the two factor states. The nonmaximal states in this context would collapse more readily and preferentially onto the factor with the greater amplitude. The analogy could be drawn here of a pencil balanced on one end in an unstable equilibrium for a maximally entangled state. The nonmaximal states could be considered as having already started falling over with a more definite direction.

The article is organized as follows: we will firstly introduce the experimental arrangement and in doing so, we will elaborate on the concept of time-bin entanglement and discuss how this differs from energy-time entanglement; we will then briefly discuss sources of errors and decoherence of pertinence to these states and optical fibre transmission; a means of characterizing the entanglement experimentally before and after transmission will then be explained. Finally, we will discuss the experimental results and conclude.

II. THE EXPERIMENT

Entangled time-bin qubits (entangled photons) [19–21] can be created, transmitted, and detected using the experimental setup pictured in Fig. 1. A coherent superposition of two classical pump pulses is generated, from a single diode laser pulse, after passing through a bulk Michelson interfer-

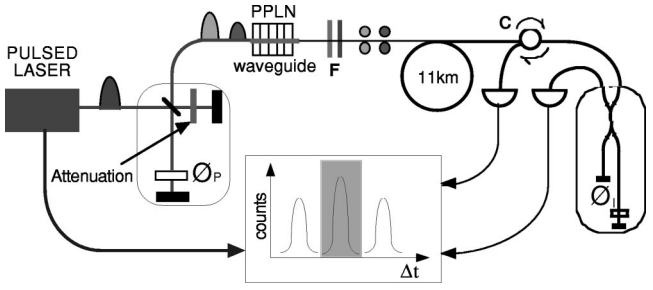

FIG. 1. Experimental schematic: A pulsed diode laser source and Michelson interferometer produce two pump pulses which are then incident on a PPLN waveguide producing two entangled photons. After filtering (F), each pair is collected and transmitted along a fiber spool to a fiber Michelson interferometer. A circulator (C) allows input and detection on the same port. A triple coincidence between two photons and one of the pump pulses then detects the entangled state.

ometer with a large path-length difference. The laser produces pulses of less than 100 ps width at a repetition rate of 80 MHz with a wavelength of 657 nm. In this scheme, the pulse duration must be short compared to the travel time difference of the pump interferometer, 1.2 ns in our case. The two pulses then undergo spontaneous parametric downconversion (SPDC) in a periodically poled lithium-niobate (PPLN) waveguide [22,23] producing pairs of entangled photon at 1314 nm wavelength, convenient for fibre telecommunication. At these wavelengths the detection is made via passively quenched germanium avalanche photodiodes, operated in Geiger mode and cooled to 77 K. Depending on the amplitudes of the two classical pulses and the relative phase ϕ_P, one can create maximally and nonmaximally entangled states of the form

$$|\psi\rangle = \alpha|1,0;1,0\rangle_{AB} + \beta e^{i\phi_P}|0,1;0,1\rangle_{AB}, \tag{1}$$

where α and β are real and $\alpha^2+\beta^2=1$, due to normalization. Our notation represents, in the case of a state like $|n,0;0,m\rangle$, that n photons are in the first time-bin for mode A and that m photons are in the second time-bin for mode B. Modes A and B are analogous to the standard idler and signal modes in SPDC. The time difference is obtained as a result of the photons having taken either the short or long arms of the bulk, or ''pump,'' interferometer. For equal amplitudes, $\alpha=\beta$, the state is maximally entangled, and when $\phi_P=0$, Eq. (1) corresponds to the maximally entangled Bell state $|\phi^+\rangle$.

After passing through the second (fiber) interferometer the state can be described by

$$\begin{aligned}|\psi'\rangle = \alpha|1,0,0;1,0,0\rangle_{AB} &+ \alpha e^{2i\phi_I}|0,1,0;0,1,0\rangle_{AB} \\ &+ \beta e^{i\phi_P}|0,1,0;0,1,0\rangle_{AB} \\ &+ \beta e^{i(2\phi_I-\phi_P)}|0,0,1;0,0,1\rangle_{AB},\end{aligned} \tag{2}$$

where ϕ_I is the relative phase between the paths of the fiber interferometer. The resulting double coincidences for the pump and A (and the pump and B) from this state correspond to the three peaks of the coincidence histogram, as depicted at the bottom of Fig. 1. The two middle terms of this state, Eq. (2), interfere with respect to the amplitudes and phases of our initial entangled state in the central time bin. We can distinguish the first and last terms in Eq. (2) via the pump timing information. Thus, conditioning the detection on events in both middle peaks by making a triple coincidence corresponds to a projective measurement onto the state of Eq. (1).

In the interests of clarity, we would like to take an aside to put time-bin entanglement [19] into some context. Time-bin entanglement is a relatively new architecture, and while some people will understand the more widely known energy-time entanglement [24], they are not the same. The difference between energy-time and time-bin entanglement is subtle but fundamental. Both procedures rely on having many photons in a coherent state pumping a nonlinear crystal. In both cases, we operate with sufficiently low power such that the probability of having more than one pump photon simultaneously undergo SPDC is negligible. In order to create entangled time-bin qubits, each pump photon corresponds to a superposition of two well-defined localizations, created by a short laser pulse and a subsequent interferometer as mentioned before. We can thus, produce pump photons in arbitrary qubit states, represented by arbitrary vectors on the Bloch sphere. Whenever one of these qubits undergoes SPDC and in conjunction with the pump pulse timing information, we finally create entangled qubits with each photon pair being in a superposition of two emission times with controllable amplitudes and relative phase Eq. (1). Conversely, energy-time entanglement originates from pump photons, from a pump laser, with a long coherence time interacting with the crystal without having passed through an interferometer. The created photon pairs are thus described by a superposition of infinitely many (and continuously distributed) emission times, only bounded by large coherence time of the pump photons.

In this experiment, we are not concerned with questions of nonlocality but simply with the robustness of the time-bin entangled states. As such we primarily utilize a ''Franson Replié'' arrangement which consists of only one analyzer interferometer as depicted in Fig. 1. This arrangement can be thought of as having used the symmetry of the standard Franson interferometer setup [25] and folded it in half, so both interferometers were on top of each other in a sense. After the 11 km of fiber (on a spool) a circulator is placed at one port of the interferometer allowing us to both input and detect. The other detector operates normally on the other port. Coincidences correspond to both photons taking the short or the long paths together as opposed to doing it in independent interferometers. While, we believe that the correlations will be the same, whether we use one or two interferometers, we will give some results with respect to an experimental arrangement with two interferometers, so that each photon travels over an independent 2.4 km length of fibre. This is done by placing a 2×2 fiber coupler (beam splitter) after the PPLN waveguide in Fig. 1, connected to the two fibers, each with an interferometer, where detection is made on one output of each.

III. SOURCES OF ERROR AND DECOHERENCE

During transmission these pure states can, in general, suffer from environment induced phase as well as from bit flips. Bit flips can happen if the broadening of the photon (in time space), due to chromatic dispersion effects in fibers, is such that the amplitude initially located in one time bin starts overlapping with the one in the other time bin, i.e., the three peaks at the bottom of Fig. 1 merge together. This reduces our ability to discriminate between them, and hence we loose information. This can be prevented in several ways: we already produce our entangled photons centered at telecommunication wavelength of 1.3 μm where chromatic dispersion is zero, thus, reducing the susceptibility to dispersion. We can improve this nonlocally by using the right choice of wavelength determined by the dispersion curve of the fibers, in the same way that it is done for energy-time entangled states [26,24]. However, note that the compensation will be

less perfect as the energy correlation between the entangled qubits is less stringent. Further on, we can utilize interference filters, in our case of 40 nm width, to reduce the spectral width of the photons, leading to a less pronounced spread of the pulse during a given transmission distance. And finally, we can increase the separation between the time bins, but this would make the interferometers larger and less stable and render the qubits more vulnerable to phase errors during transmission.

Phase errors generally arise as a result of some random variation between the two time bins but this is negligible in our case, at least as far as transmission is concerned. With 1.2 ns separation between time bins, there would need to be very high frequency (GHz) noise in order to produce a phase flip. Our main phase error arises during creation and detection of ensembles of photons over extended periods of time. This requires that the interferometers have the same path-length difference for the entire time that we prepare and measure a particular state. This will be discussed in further detail in connection with the experimental analysis.

IV. ROBUST ENTANGLEMENT

If we are going to generate nonmaximally entangled states, then an important question is: how can we characterize them? Firstly, we can restrict our attention to pure states of the form of Eq. (1), as we postselect the final state. Now, given the state of Eq. (2), the probability of coincidence in the central time bin is given by

$$P_c = 0.5[\alpha^2 + \beta^2 + 2\alpha\beta\cos\phi]. \tag{3}$$

We see that the probability of a coincidence detection varies with the phase $\phi = 2\phi_I - \phi_P$. Therefore, by varying the phase, we can scan through maximum and minimum probabilities corresponding to regimes of maximum constructive and destructive interference and thus determine the visibility which is given by

$$V = 2\alpha\beta. \tag{4}$$

Our fiber interferometers are thermally stabilized and the phase is varied by changing the temperature of the interferometer.

In Fig. 2, we see the results of this approach using the experimental setup in Fig. 1 with 11 km of fiber. Due to the long distances the signal is reduced and hence, we have to count for a long time, 60 s in this instance. The squares denote the number of triple coincidences in each 60 s interval. It is for this 60 s integration time that we have to maintain the stability of the laser to within a fraction of a wavelength to minimize the phase errors discussed previously. The solid line that traces these points is a sinusoidal fit to the data derived from Eq. (3) and allows us to determine the visibility.

The key here is that the net visibility parametrizes the entanglement in the final state. Both the bit flips and phase flips will manifest themselves as a reduction in visibility and as such, we will use this as the experimental measure of our entanglement. A visibility greater than 71% is commonly

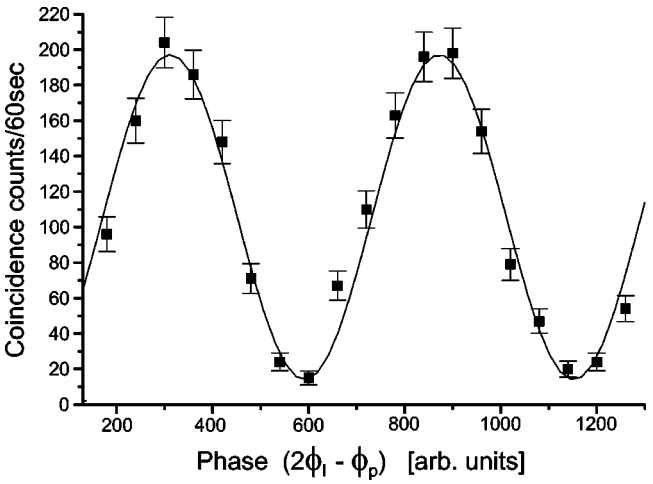

FIG. 2. The interference fringes for the experimental setup shown in Fig. 1 after the photons had travelled 11 km.

associated with nonlocality in Bell experiments. With respect to Fig. 2, this analysis returns a net visibility of $V = 94.2 \pm 4.8\%$ after transmitting the maximally entangled state over 11 km. The error in this result, ΔV, is determined by the numerical uncertainty in the sinusoidal fit to the data.

Table I shows the raw visibility as well as the net visibility, which is derived after subtracting the accidental coincidences, for maximally entangled states with both one and two interferometers. We see that although the raw visibility is less over the longer distances, the net visibilities are almost equivalent.

Let us briefly comment on the nature of accidental coincidences. They occur if both events in the coincidence window are triggered by noise. Also, there will be contributions if one photon triggers one detector and noise triggers the other while the photon's correlated partner is absorbed in the fiber or not detected. Thus, the resulting decrease of raw visibility is due to a combination of fiber losses and detector noise. However, since we are interested in the impact of bit and phase flips on the entanglement, we must subtract this source of noise which is well understood and is easily measured.

The other aspect of characterization is related to generating the nonmaximally entangled states. We can quantify the expected entanglement in the state in terms of the entropy of entanglement:

$$E = -\alpha^2 \log_2 \alpha^2 - (1-\alpha^2)\log_2(1-\alpha^2), \tag{5}$$

TABLE I. The raw and net (accidental coincidences subtracted) visibilities for the maximally entangled states. I and II use one interferometer and rows III and IV use two. ΔV is the uncertainty in the visibility.

Run	Distance	V_{raw}	V_{nett}	ΔV
I	0 km	90.2	94.9	3.7
II	11 km	86.8	94.2	4.8
III	0 km	89.1	92.7	4.7
IV	2.4 km	84.5	92.2	4.8

where we use the amplitudes of the two pump pulses, appropriately normalized. With this experimental setup nonmaximally entangled states can be realized in a controlled manner by varying the attenuation in one of the arms of the pump interferometer, so that the classical pulses have unequal magnitudes. In practice, we vary the attenuation in both arms so that we have the same mean power before the waveguide.

In this experiment, we use a PPLN waveguide which is a high efficiency generator of entangled photons. A consequence of this high efficiency, conversion rates four orders of magnitude higher than obtained with bulk sources [22,23], is that, when using a pulsed laser, the probability of producing multiple photon pairs per pulse can become significant. This has the effect of reducing the interference visibility and hence at a more fundamental level the entanglement. This is a critical point especially in experiments of this nature. We ensured that we had the same mean power at the PPLN waveguide throughout these experiments. This was done so that any reduction in the visibility was due to decoherence and not due to variation in the rate of production of photon pairs.

The results of the measurements of the nonmaximally entangled states are given in Fig. 3. The solid line shows the theoretically expected visibility from Eq. (4), measured after transmission, as a function of the entanglement Eq. (5), measured before transmission, as α and β are varied. In the experiment, we have complete control over the classical amplitudes and these are measured directly at the output of the pump interferometer. After transmission the net visibility are obtained from sinusoidal fits described previously. On average, subtraction of the noise improved the raw visibilities for the zero-distance runs by less than 5% and the 11 km runs by less than 9%. A dashed line corresponding to the theory but scaled to have a maximum visibility of 95% is also shown. We see that for both the experimental setup as depicted in Fig. 1, with or without 11 km of fiber, and also with one or with two interferometers the results are in good agreement with the theory. Specifically, we see that regardless of the initial entanglement or the distance travelled that there is no loss of entanglement over transmission for any of the states.

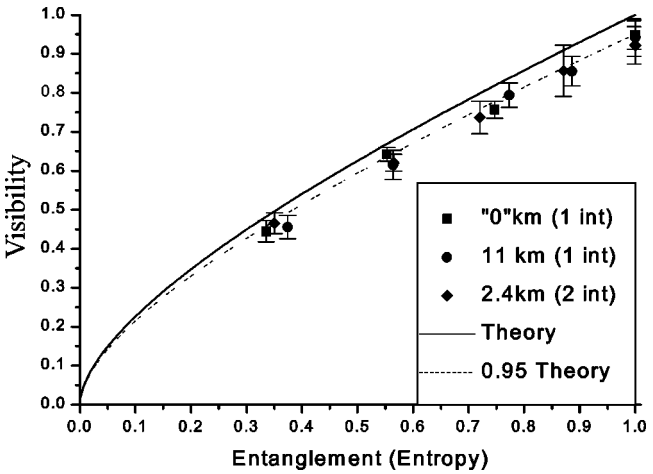

FIG. 3. Net visibility of the output state as a function of the expected entanglement, measured at our source. The relationship is unchanged by transmission over significant distances.

V. CONCLUSION

We have shown that one can generate, in a controlled way, true-qubit states with arbitrary degrees of entanglement using a pulsed diode laser and a PPLN waveguide. We have also shown the transmission of entangled qubits over distances of interest for distributed quantum communication. This is a technology under development which holds great promise for integrated quantum optics and hence for quantum communication. We note that the results do not indicate any behavior indicative of spontaneous collapse over these large distances. The main results proved resoundingly that the entanglement of time-bin qubits is robust with transmission distances up to 11 km.

ACKNOWLEDGMENTS

This work was supported by the Swiss NCCR ''Quantum Photonics'' and the European QuComm IST projects. W.T. acknowledges funding by the ESF Program Quantum Information Theory and Quantum Computation (QIT).

[1] See for instance, M.A. Nielsen and I.L. Chuang, *Quantum Computation and Quantum Information* (Cambridge University Press, Cambridge, 2001).
[2] W. Tittel and G. Weihs, Quantum Inf. Comput. **1**, 3 (2001).
[3] A. Einstein, B. Podolski, and N. Rosen, Phys. Rev. Lett. **47**, 1215 (1935).
[4] J.S. Bell, *Speakable and Unspeakable in Quantum Mechanics* (Cambridge University Press, Cambridge, 1987).
[5] A. Aspect, J. Dalibard, and G. Roger, Phys. Rev. Lett. **49**, 1804 (1982).
[6] W. Tittel, J. Brendel, H. Zbinden, and N. Gisin, Phys. Rev. Lett. **81**, 3563 (1998).
[7] G. Weihs *et al.*, Phys. Rev. Lett. **81**, 5039 (1998).
[8] A.K. Ekert, Phys. Rev. Lett. **67**, 661 (1991).
[9] N. Gisin, G. Ribordy, W. Tittel, and H. Zbinden, Rev. Mod. Phys. **74**, 145 (2002).
[10] C.H. Bennett *et al.*, Phys. Rev. Lett. **70**, 1895 (1993).
[11] D. Bouwmeester *et al.*, Nature (London) **390**, 575 (1997).
[12] D. Boschi *et al.*, Phys. Rev. Lett. **80**, 1121 (1998).
[13] Y.H. Kim, S.P. Kulik, and Y. Shih, Phys. Rev. Lett. **86**, 1370 (2001).
[14] J.I. Cirac, P. Zoller, H.J. Kimble, and H. Mabuchi, Phys. Rev. Lett. **78**, 3221 (1997).
[15] H.J. Briegel, W. Dur, J.I. Cirac, and P. Zoller, Phys. Rev. Lett. **81**, 5932 (1998).
[16] T. Jennewein, C. Simon, G. Weihs, H. Weinfurter, and A. Zeilinger, Phys. Rev. Lett. **84**, 4729 (2000).
[17] W.H. Furry, Phys. Rev. **49**, 393 (1936).
[18] G.C. Ghirardi, A. Rimini, and T. Weber, Phys. Rev. D **34**, 470 (1986).
[19] J. Brendel, N. Gisin, W. Tittel, and H. Zbinden, Phys. Rev. Lett. **82**, 2594 (1998).

[20] W. Tittel, J. Brendel, H. Zbinden, and N. Gisin, Phys. Rev. Lett. **84**, 4737 (2000).
[21] W. Tittel, H. Zbinden, and N. Gisin, Phys. Rev. A **63**, 042301 (2001).
[22] S. Tanzilli *et al.*, Electron. Lett. **37**, 28 (2001).
[23] S. Tanzilli *et al.*, Eur. Phys. J. D **18**, 155 (2002).
[24] W. Tittel, J. Brendel, N. Gisin, and H. Zbinden, Phys. Rev. A **59**, 4150 (1999).
[25] J.D. Franson, Phys. Rev. Lett. **62**, 2205 (1989).
[26] J.D. Franson, Phys. Rev. A **45**, 3126 (1992).